



AFRL-RZ-WP-TP-2007-247

THE EFFECT OF STEADY FLUID MOTION ON ONE-DIMENSIONAL WAVE PROPAGATION (POSTPRINT)

Barry Kiel

**Combustion Branch
Turbine Engine Division**

AUGUST 2007

Approved for public release; distribution unlimited.

See additional restrictions described on inside pages

STINFO COPY

**AIR FORCE RESEARCH LABORATORY
PROPULSION DIRECTORATE
WRIGHT-PATTERSON AIR FORCE BASE, OH 45433-7251
AIR FORCE MATERIEL COMMAND
UNITED STATES AIR FORCE**

REPORT DOCUMENTATION PAGE				<i>Form Approved</i> OMB No. 0704-0188	
<p>The public reporting burden for this collection of information is estimated to average 1 hour per response, including the time for reviewing instructions, searching existing data sources, gathering and maintaining the data needed, and completing and reviewing the collection of information. Send comments regarding this burden estimate or any other aspect of this collection of information, including suggestions for reducing this burden, to Department of Defense, Washington Headquarters Services, Directorate for Information Operations and Reports (0704-0188), 1215 Jefferson Davis Highway, Suite 1204, Arlington, VA 22202-4302. Respondents should be aware that notwithstanding any other provision of law, no person shall be subject to any penalty for failing to comply with a collection of information if it does not display a currently valid OMB control number. PLEASE DO NOT RETURN YOUR FORM TO THE ABOVE ADDRESS.</p>					
1. REPORT DATE (DD-MM-YY) August 2007		2. REPORT TYPE Conference Paper Postprint		3. DATES COVERED (From - To) 01 August 2005 – 01 August 2007	
4. TITLE AND SUBTITLE THE EFFECT OF STEADY FLUID MOTION ON ONE-DIMENSIONAL WAVE PROPAGATION (POSTPRINT)				5a. CONTRACT NUMBER In-house	
				5b. GRANT NUMBER	
				5c. PROGRAM ELEMENT NUMBER 62203F	
6. AUTHOR(S) Barry Kiel (AFRL/RZTC) Reza Kashani, Ph.D. (University of Dayton)				5d. PROJECT NUMBER 3066	
				5e. TASK NUMBER 05	
				5f. WORK UNIT NUMBER 306605YY	
7. PERFORMING ORGANIZATION NAME(S) AND ADDRESS(ES) Combustion Branch (AFRL/RZTC), Turbine Engine Division Air Force Research Laboratory, Propulsion Directorate Wright-Patterson Air Force Base, OH 45433-7251 Air Force Materiel Command, United States Air Force				University of Dayton Department of Mechanical and Aerospace Engineering Dayton, OH	
9. SPONSORING/MONITORING AGENCY NAME(S) AND ADDRESS(ES) Air Force Research Laboratory Propulsion Directorate Wright-Patterson Air Force Base, OH 45433-7251 Air Force Materiel Command United States Air Force				8. PERFORMING ORGANIZATION REPORT NUMBER AFRL-RZ-WP-TP-2007-247	
				10. SPONSORING/MONITORING AGENCY ACRONYM(S) AFRL/RZTC	
				11. SPONSORING/MONITORING AGENCY REPORT NUMBER(S) AFRL-RZ-WP-TP-2007-247	
12. DISTRIBUTION/AVAILABILITY STATEMENT Approved for public release; distribution unlimited.					
13. SUPPLEMENTARY NOTES Conference paper published in the Proceedings of the 45th AIAA Aerospace Sciences Meeting and Exhibit. The U.S. Government is joint author of this work and has the right to use, modify, reproduce, release, perform, display, or disclose the work. PAO Case Number: AFRL/WS 07-0001, 04 Jan 2007.					
14. ABSTRACT Reduced order modeling of thermoacoustic instabilities involves the coupled modeling of the wave propagation in the combustion chamber and the unsteady heat release. In many combustion systems the Mach number is low enough that the effect of the fluid motion on the wave propagation can be ignored. Ignoring the fluid motion results in the use of the wave equation to model the wave motion in the combustion chamber. In a previous paper the momentum and pressure equations were linearized by representing the fluid motion by a steady Mach number. In that research the frequency and phase relationship change as Mach number increases. In this research unsteady fluid motion is considered. The governing equations for momentum and pressure are modeled in SIMULINK and studied using frequency response tools.					
15. SUBJECT TERMS					
16. SECURITY CLASSIFICATION OF:			17. LIMITATION OF ABSTRACT: SAR	18. NUMBER OF PAGES 18	19a. NAME OF RESPONSIBLE PERSON (Monitor) Lt. Kyle Garwick 19b. TELEPHONE NUMBER (Include Area Code) N/A
a. REPORT Unclassified	b. ABSTRACT Unclassified	c. THIS PAGE Unclassified			

The Effect of Steady Fluid Motion on One-Dimensional Wave Propagation

Barry Kiel
Air Force Research Laboratory
Wright Patterson Air Force Base

Reza Kashani, Ph.D.
Department of Mechanical and Aerospace Engineering
University of Dayton
Dayton, OH

ABSTRACT

Reduced order modeling of thermoacoustic instabilities involves the coupled modeling of the wave propagation in the combustion chamber and the unsteady heat release. In many combustion systems the Mach number is low enough that the effect of the fluid motion on the wave propagation can be ignored. Ignoring the fluid motion results in the use of the wave equation to model the wave motion in the combustion chamber. In a previous paper the momentum and pressure equations were linearized by representing the fluid motion by a steady Mach number. In that research the frequency and phase relationship change as Mach number increases. In this research unsteady fluid motion is considered. The governing equations for momentum and pressure are modeled in SIMULINK and studied using frequency response tools.

1 INTRODUCTION

Combustion instability manifests itself in many of today's combustors. Instabilities have been reported in all types of propulsion systems including rockets, scramjets and gas turbine combustors and augmentors. Throughout the 50 year development of high performance gas turbine engines combustion instability has always been a major challenge for both the combustor and the thrust augmentor. Over the same time period many advances in modeling combustion instability have been made.

Traditional thermoacoustics modeling is based on Culick's framework, (Candel 2002, Malhotra 2004). In this framework pressure fluctuations are assumed to be small and the Mach number of the flow in the combustion chamber are assumed to be small. These assumptions result in wave equation that describes the wave propagation in the

combustion chamber forced by an unsteady heat release term. This type of model has proven very effective in systems where the Mach number is small.

The study of duct flows for the inlet of gas turbine engines has shed significant light on the effect of steady fluid motion on wave propagation in ducts where fluid motion was appreciable, Morse and Ingard (1968), Eversman (1970, 1971b), Ingard and Singhai (1973, 1974), Gogate and Munjal (1992), and Dokumaci (1995). The conclusion drawn from much of this research is the wave equation does not accurately capture the wave motion in the duct when there is appreciable fluid motion. Instead a more complex second order PDE is required to capture the effect of the fluid motion.

In this paper the effect of unsteady fluid motion is studied. The wave propagation is modeled using finite difference in the SIMULINK environment. The steady pressure and momentum equations are modeled using finite difference to reduce them to a set of ODE's. These ODEs are then analyzed using the frequency response tools available in MATLAB. Bode plots and pole zero plots are constructed over a wide range of operating conditions. These plots are then compared to previous research where the pressure and momentum equations were simplified by assuming the fluid motion could be represented by a steady Mach number.

2 WAVE PROPAGATION MODELS

2.1. Governing Equations

The governing equations for wave propagation are derived from the continuity and momentum equations. The steady flow model is derived assuming inviscid flow, with no body forces. The governing equations for continuity and momentum reduce to:

$$\frac{\partial \rho}{\partial t} = -\rho \frac{\partial u}{\partial x} - u \frac{\partial \rho}{\partial x} \quad (2-1)$$

$$\rho \frac{\partial u}{\partial t} + \rho u \frac{\partial u}{\partial x} = -\frac{\partial p}{\partial x} \quad (2-2)$$

Equation 2-1 is further reduced by assuming that, for an isentropic fluid, pressure and density are related by:

$$\partial p = a^2 \partial \rho \quad (2-3)$$

The pressure equation can also be derived from the energy equation when isentropic flow is assumed, see appendix 1. Equation 2-1 then reduces to:

$$\frac{\partial p}{\partial t} = -a^2 \rho \frac{\partial u}{\partial x} - u \frac{\partial p}{\partial x} \quad (2-4)$$

2.2 Wave Propagation Models

Equations 2-2 and 2-4 are used as the governing equations for both the Homogenous Wave and Steady Flow Models. Equation 2-2 can also be modified with the continuity equation to give an alternate momentum equation. This methodology was applied by Morse and Ingard (1968) to achieve a second order PDE that was a function of pressure only. See Appendix 2 for the derivation of Equation 2-5.

$$\rho \frac{\partial u}{\partial t} = \frac{u}{a^2} \frac{\partial p}{\partial t} + \left(\frac{uu}{a^2} - 1 \right) \frac{\partial p}{\partial x} \quad (2-5)$$

The final wave propagation models are derived by assuming the flow through the duct is steady and thus the mean is constant. The models are derived by assuming the velocity which multiplies the derivatives on the right hand side of Equations 2-4 and 2-5 is steady and can be represented with Mach number by:

$$u = Ma \quad (2-6)$$

Substituting Equation 2-6 into Equations 2-4 and 2-5 results in:

$$\frac{\partial p}{\partial t} = -a^2 \rho \frac{\partial u}{\partial x} - Ma \frac{\partial p}{\partial x} \quad (2-7)$$

$$\rho \frac{\partial u}{\partial t} = \frac{M}{a} \frac{\partial p}{\partial t} + [M^2 - 1] \frac{\partial p}{\partial x} \quad (2-8)$$

Equations 2-7 and 2-8 are termed the Steady Flow Model. The Homogenous Wave Model is obtained by assuming that the Mach number is zero. Applying this assumption results in:

$$\frac{\partial p}{\partial t} = -a^2 \rho \frac{\partial u}{\partial x} \quad (2-9)$$

$$\rho \frac{\partial u}{\partial t} = -\frac{\partial p}{\partial x} \quad (2-10)$$

2.3 Second Order Equations for Pressure

The equations in both models can be combined to formulate second order PDEs with pressure as the only dependant variable. This is accomplished by taking the temporal derivative of the pressure equation and the spatial derivative of the momentum equation, and then substituting the derivative momentum equation into the derivative pressure equation. Also required is the assumptions:

1) Constant Properties

2) $\partial p \gg \partial \rho$

For the Homogenous Wave Model the result is:

$$\frac{\partial^2 p}{\partial t^2} = -a^2 \rho \frac{\partial^2 u}{\partial x \partial t} \quad (2-11)$$

$$\rho \frac{\partial^2 u}{\partial t \partial x} = -\frac{\partial^2 p}{\partial x^2} \quad (2-12)$$

Making the final substitution:

$$\frac{\partial^2 p}{\partial t^2} - a^2 \frac{\partial^2 p}{\partial x^2} = 0 \quad (2-13)$$

A second order PDE for pressure is found for the Steady Flow Model, Equations 2-7 and 2-8, by applying the same assumptions and derivatives:

$$\frac{\partial^2 p}{\partial t^2} = -a^2 \rho \frac{\partial^2 u}{\partial x^2} - Ma \frac{\partial^2 p}{\partial x^2} \quad (2-14)$$

$$\rho \frac{\partial^2 u}{\partial t \partial x} = \frac{M}{a} \frac{\partial^2 p}{\partial t \partial x} + [M^2 - 1] \frac{\partial^2 p}{\partial x^2} \quad (2-15)$$

Substituting Equation 2-15 into 2-14, the second order PDE for pressure is:

$$\frac{\partial^2 p}{\partial t^2} + a2M \frac{\partial^2 p}{\partial x \partial t} - a^2(1 - M^2) \frac{\partial^2 p}{\partial x^2} = 0 \quad (2-17)$$

Equation 2-13 should be recognized as the Homogenous Wave Equation. Equation 2-17 is often termed the convective wave equation, Morse and Ingard (1968) and Dowling (2003)

3. SIMPLIFICATION OF PDEs TO ODE's WITH SECOND ORDER ACCURATE FINITE DIFFERENCE

The first order equations for the Homogenous Wave Model and Steady Flow Model are simplified from PDEs to ODEs by using finite difference. The domain is broken down into n nodes. At each node the spatial derivatives are simplified using second order accurate finite difference operators. For the central nodes the second order finite difference operator for any variable v is:

$$\frac{\partial v}{\partial x} = \frac{v(x + \Delta x, y) - v(x - \Delta x, y)}{2\Delta x} + O(\Delta x^2) \quad (3-1)$$

For the end nodes the operators are:

$$\frac{\partial v}{\partial x} = \frac{-3v(x, y) + 4v(x + \Delta x, y) - v(x + 2\Delta x, y)}{2\Delta x} + O(\Delta x^2)$$

$$\frac{\partial v}{\partial x} = \frac{3v(x, y) - 4v(x - \Delta x, y) + v(x - 2\Delta x, y)}{2\Delta x} + O(\Delta x^2)$$

Applying the central difference to the Homogenous Wave Model Equations 2-9, and 2-10 become:

$$\frac{\partial p}{\partial t} = -\frac{a^2 \rho}{2\Delta x} (u_{i+1} - u_{i-1}) \quad (3-2)$$

$$\rho \frac{\partial u}{\partial t} = -\frac{1}{2\Delta x} (p_{i+1} - p_{i-1}) \quad (3-3)$$

Applying the central difference to the Steady Flow Model results in:

$$\frac{\partial p}{\partial t} = -\frac{a^2 \rho}{2\Delta x} ((u)_{i+1} - (u)_{i-1}) - \frac{Ma}{2\Delta x} ((p)_{i+1} - (p)_{i-1}) \quad (3-4)$$

$$\rho \frac{\partial u}{\partial t} = \frac{M}{a} \frac{\partial p}{\partial t} + \frac{[M^2 - 1]}{2\Delta x} ((p)_{i+1} - (p)_{i-1}) \quad (3-5)$$

4. BOUNDARY CONDITIONS

The natural frequencies of a one dimensional tube will differ depending on the boundary conditions (Richardson (1949), Wood (1957)). Depending on the type of boundary the pressure and velocity will either be a node or anti-node at the boundary. Since acoustic pressure and acoustic velocity are sinusoidal, a node is defined as the point where the sinusoid is zero. An anti-node is defined as the point where the sinusoid is maximum. Further, if a node occurs at a boundary the reflected wave's phase will be preserved. For an anti-node at a boundary, the reflected wave's phase changes by 180 degrees.

For ducts without flow, there are two types of boundaries in the extreme, acoustically closed and acoustically open. For an acoustically closed boundary the acoustic velocity must be zero at the boundary, thus the magnitude of the acoustic pressure must be maximum. Since the waves are sinusoidal, if the acoustic pressure is maximum, the derivative of the acoustic pressure must be zero (Pota, and Kelkar (2001)). At the acoustically open boundary the acoustic pressure must be a minimum at the boundary, thus the acoustic velocity is maximum. Since the velocity is also sinusoidal, if the acoustic velocity is a maximum, the derivative of the acoustic velocity must be zero. Applying the boundaries to the Homogenous Wave Equation the natural frequencies can be obtained. For a duct with open-open or closed-closed boundaries the natural frequencies are:

$$w = \frac{na}{2L} \quad (4-1)$$

For a duct with closed-open or open-closed boundary the natural frequencies are:

$$w_{\substack{c-o \\ o-c}} = \frac{(2n-1)a}{4L} \quad (4-2)$$

5. COMPUTATIONAL DOMAIN

The computational domain in this study is a one-dimensional duct whose length is 1.5 meters. At the inlet of the duct, on the left, a closed boundary will be imposed. At the exit of the duct, on the right, an open boundary will be imposed. The duct will contain vitiated air whose temperature is approximately 1500K. This temperature results in a wave speed of approximately 925 m/s and a ratio of specific heats of 1.3. Table 5-1 is a list of the first 10 natural frequencies of the duct assuming no fluid motion.

N	C-O Boundary
1	154.17
2	462.50
3	770.83
4	1079.17
5	1387.50
6	1695.83
7	2004.17
8	2312.50
9	2620.83
10	2929.17

Table 5-1 Theoretical Natural Frequencies for a 1.5 m Closed-Open Tube with 925 m/s Wave Speed

6 COMPARISON OF HOMOGENOUS WAVE AND STEADY FLOW MODELS FREQUENCY RESPONSE

6.1 Homogenous Wave Model Results

The computational domain was modeled using SIMULINK. For the Homogenous Wave Model the first order ODEs, Equations 3-2 and 3-3 were applied to 9 interior nodes. On the first and last nodes the boundary conditions were applied, and the remaining spatial derivatives were treated with the upwind and downwind second order first derivatives. This system was then analyzed using frequency-response methods in SIMULINK.

Frequency-response methods are the most convenient methods for engineers to analyze linear systems. In these methods, the steady state response of a sinusoidal input to a system is found. The input is swept over a user defined range of frequencies. The results of these methods are reported in many ways. In this research the results of the frequency

response analysis are reported with semi-logarithmic plots called Bode magnitude and phase plots. For more information on this method and Bode plots please refer to Ogata (1970).

Figure 6-1 is a plot of the magnitude of the frequency response, or Bode Magnitude Plot, of the Homogenous Wave Model with closed-open boundaries. Unless otherwise stated the input point is always the first node and the output point the last computational node. Figure 6-2 is the Bode Magnitude plot for

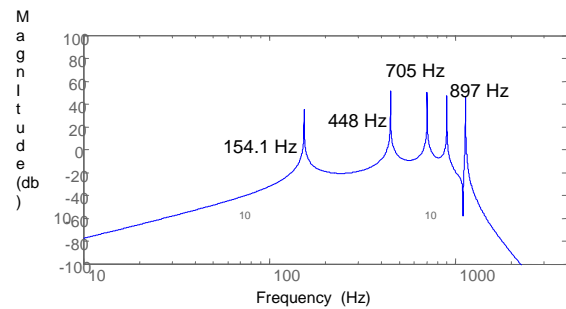


Figure 6-1 Bode Magnitude Plot for the Homogenous Wave Model, Closed-Open Boundaries

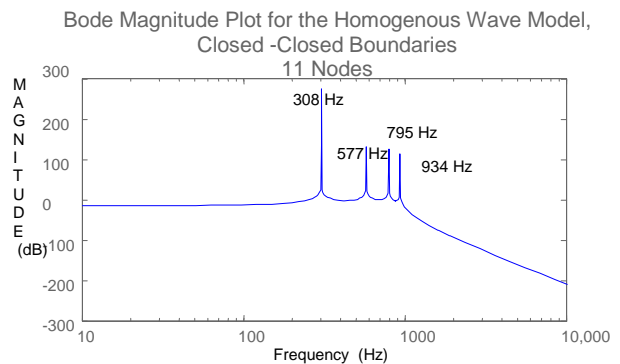


Figure 6-2 Bode Magnitude Plot for the Homogenous Wave Model, Closed-Closed Boundaries

closed-closed boundaries. In both plots there are 5 peaks in the plot at 5 distinct frequencies. These are the frequencies where the model is

most sensitive to the sinusoidal input, commonly referred to as the natural frequencies.

Table 6-1 lists the theoretical and modeled natural frequencies for the Homogenous Wave Model. It lists the results for both a closed-open and a closed-closed system. In both cases the finite difference model accurately resolves the first frequency to within less than 1%. For the higher frequency natural frequencies the mode does not compare a well with >15% error in the 4th natural frequencies for both the closed-open and closed-closed models.

n	C-O	11 Nodes	Error	C-C	11 Nodes	Error
1	154.17	154.10	0.04	308.33	308.00	0.11
2	462.50	448.00	3.14	616.67	577.00	6.43
3	770.83	705.00	8.54	925.00	795.00	14.05
4	1079.17	897.00	16.88	1233.33	934.00	24.27

Table 6-1 Theoretical and Modeled Natural Frequencies for 11 Node Closed-Open and Closed-Closed Homogenous Wave Models

Figure 6-3 depicts the Bode Magnitude Plot for the Homogenous Wave Model with 49

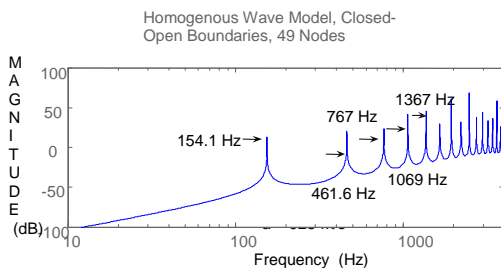


Figure 6-3 Bode Magnitude Plot for the Homogenous Wave Model, Closed-Open Boundaries, 49 Computational Nodes

computational nodes. Table 6-2 lists the theoretical frequencies and the modeled results for 11 and 49 computational nodes. Note that as the number of nodes increases the accuracy of the model increases tremendously. For the 49 node model the first four natural frequencies are predicted to within less than 1% error.

n	C-O	11 Nodes	error	49 Nodes	error
---	-----	----------	-------	----------	-------

1	154.17	154.10	0.04	154.1	0.04
2	462.50	448.00	3.14	461.7	0.17
3	770.83	705.00	8.54	767.2	0.47
4	1079.17	897.00	16.88	1069.2	0.92
5	1387.50			1365.5	1.59
6	1695.83			1657.5	2.26
7	2004.17			1940.1	3.20
8	2312.50			2215.8	4.18
9	2620.83			2480.5	5.35
10	2929.17			2733.9	6.67

Table 6-2 Theoretical and Modeled Natural Frequencies for Closed-Open Homogenous Wave Models

6.2 Steady Flow Model Results

The domain was modeled employing the Steady Flow Model with 49 computational nodes. In this model the fluid motion is considered to have a constant mean and is thus modeled by a constant wave speed and Mach number. Figure 6-4 depicts the Bode magnitude plot for the Homogenous Wave Model, blue, and The Steady Flow Model with Mach number equal 0.4, purple. Several things can be noted from this plot. The first is that the natural frequencies are shifted to the left, or decrease by over 15 Hz. The second is that the magnitude increases over 40 decibels (db). Finally in the plot for $M = 0.4$ there is a second peak with lower amplitude a few hertz larger than the first for each natural frequency.

The shift of the natural frequency to the right is addresses first. Figure 6-4 depicts the Bode Magnitude plot for the Homogenous Wave Model and the Steady Flow Model with Mach numbers ranging from 0.1 to 0.4. When the first natural frequency at each Mach number is compared to the Homogenous Wave Model the frequencies vary by:

$$\omega_{nSF} = \omega_{nHW} (1 - M^2)$$

This result can be explained when the result is considered in light of the second order PDEs for both of the models, repeated here

$$\frac{\partial^2 p}{\partial t^2} - a^2 \frac{\partial^2 p}{\partial x^2} = 0 \quad (2-13)$$

$$\frac{\partial^2 p}{\partial t^2} + a2M \frac{\partial^2 p}{\partial x \partial t} - a^2(1 - M^2) \frac{\partial^2 p}{\partial x^2} = 0 \quad (2-17)$$

When comparing the second spatial derivative of each equation, the wave speed in the Steady Flow Model is modified ($1-M^2$). Thus one would expect that the natural frequency is modified by the same factor. This is further born out in Figure 6-5.

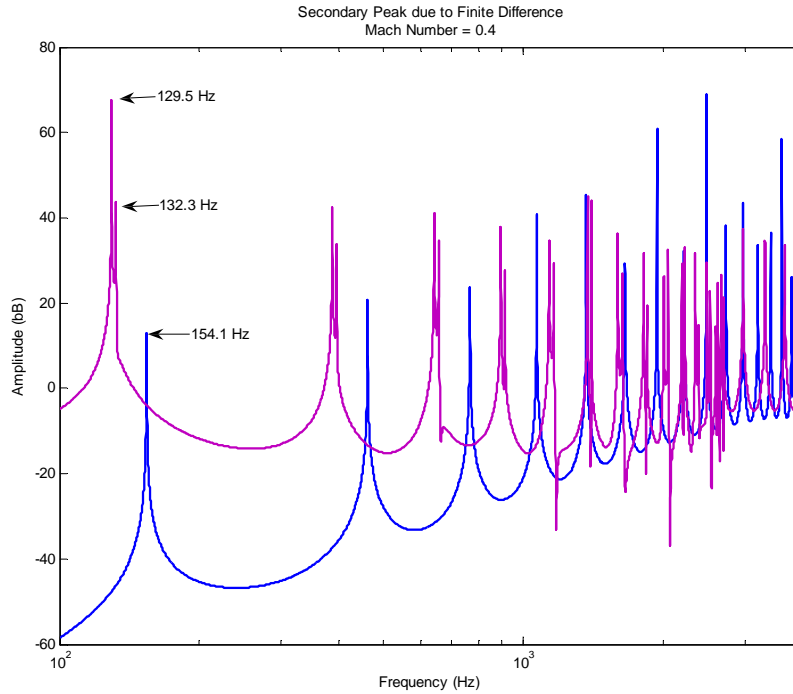


Figure 6-4 Bode Magnitude Plot for the Homogenous Wave Mode (blue, and the Steady Flow Model, (Purple) with Closed-Open Boundaries, 49 Computational Nodes

In figure 6-5 the resultant steady state frequency response is plotted for a range of Mach numbers. In each case the first natural frequency is modified by $(1-M^2)$.

The secondary peaks in Figures 6-4 and 6-5 can be explained when finite difference is considered. For the Homogenous Wave Model the first natural frequency is:

$$w_n = \frac{a}{4(n-1)\Delta x}$$

For the Steady Flow Model Figures 6-4 and 6-5 indicate the new natural frequency is

$$w_{n(new)} = \frac{a(1-M^2)}{4(n-1)\Delta x}$$

The frequency of the second peak, though, is:

$$w_{n2} = \frac{a(1-M^2)}{4(n-2)\Delta x}$$

The second peak probably occurs because a central difference is used on the center 9 points while upwind/downwind differences are used on the boundaries. Thus the second peak is the natural frequency if the central nodes are only considered. Another explanation for the second peak could be a reflection from one of the boundary conditions.

Figure 6-5 depicts the phase relationship for the forward (blue) and rearward (green) waves. The “forward traveling wave” phase relationship is obtained by using the inlet

as the input and outlet as the output for the frequency

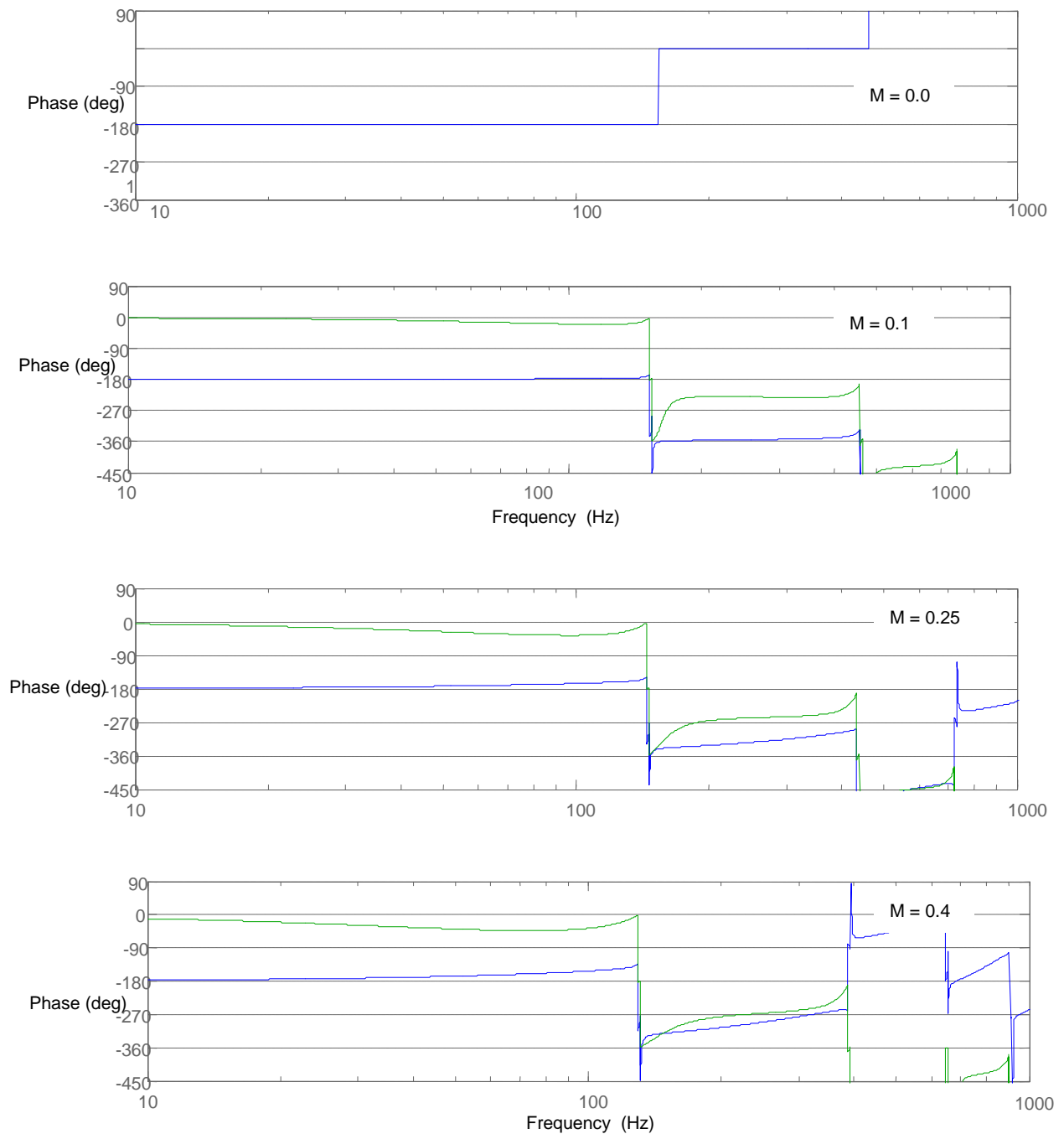


Figure 6-5 The Effect of Mach Number on the Phase of the Forward and Backward Wave Propagation

response calculation. The green line, or “rearward traveling wave”, is obtained by

using the inlet as the output and outlet as

the input for the frequency response calculation.

The first phase plot depicts the Homogenous Wave Model, $M = 0.0$. Note there is only a blue curve for this plot. This is because the forward and rearward waves each have the same amplitude and phase relationship. Mathematically the forward and rearward waves combine to form a standing wave. In this plot the phase is -180 degrees for frequencies less than the natural frequency. The phase then increases by 180 degrees at the natural frequency. It is then constant again until the next natural frequency where it again increases by 180.

Equation 6-1 is a simple second order transfer function. The frequency response of

$$\frac{1}{s^2 + 1} \quad (6-1)$$

this system is displayed in the Bode Magnitude/Phase plot, Figure 6-6. For this system there is a step change in the phase of 180 degrees at the natural frequency of the system. The phase relationship for the Homogenous Wave Model at the natural frequency is indicative of that of a second order system.

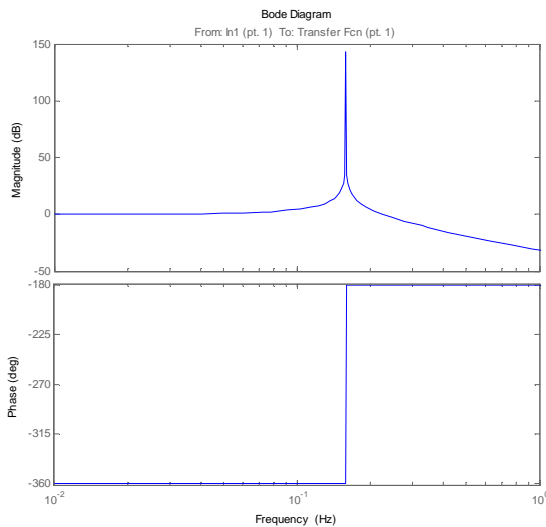


Figure 6-6 Bode Magnitude/Phase Plot for the Simple Second Order System, Eqn. 6-1

The second, third and fourth phase plots are for Mach numbers 0.1, 0.25, and 0.4 respectively. In each case the forward traveling and rearward traveling waves have very different phase relationships than the Homogenous Model. In each case the phase of rearward traveling wave is increased by 180 degrees relative to the forward traveling wave at low frequency. As the input frequency is increased the phase of the forward traveling wave increases while that of the rearward traveling wave decreases. Near the natural frequency the phase of the forward traveling wave continues to increase and the phase of the rearward traveling wave changes sign and also begins to increase. At the natural frequency, the forward traveling wave's phase changes by -180 degrees, while the rearward traveling wave's frequency changes by -360 degrees.

Equation 6-2 is a damped second order system with a zero and two poles at the origin.

$$\frac{1}{s^2} \frac{s + a}{s^2 + 2\zeta s + a} \quad (6-2)$$

The frequency response of this transfer function is depicted in Figure 6-7. Figure 6-8 is the frequency response of the Steady Flow Model with Mach number = 0.4. Note the phase portion of the forward traveling wave, blue, Figure 6-8 has the same shape as the phase of Figure 6-2

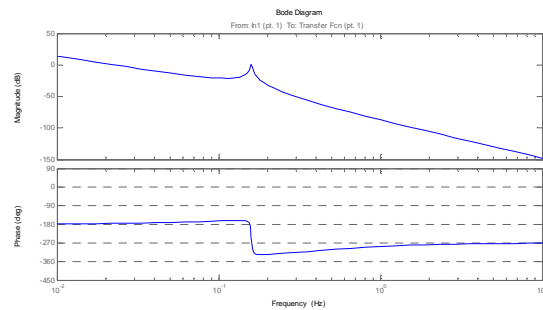


Figure 6-7 Bode Plot of Equation 6-2

Equation 6-3 has two damped second order systems with similar natural

frequency multiplied by a pole and zero. Figure 6-9 is

$$\frac{1}{s+b} \frac{s+a}{s^2+2\zeta s+c} \frac{1}{s^2+2\zeta s+d} \quad (6-3)$$

$c \sim d > a > b$

the Bode plot for Equation 6-3. Comparing the phase plot of Figure 6-9 to that of the backward traveling wave in Figure 6-8 they both have similar shape. In both cases the phase is near zero for low frequency, decreases, then increases as the frequency increases to the natural frequency. At the natural frequency the phase goes through -360.

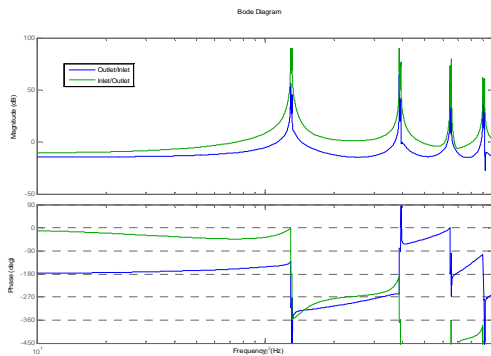


Figure 6-8 Bode Plot of the Steady Flow Model with Mach Number 0.4

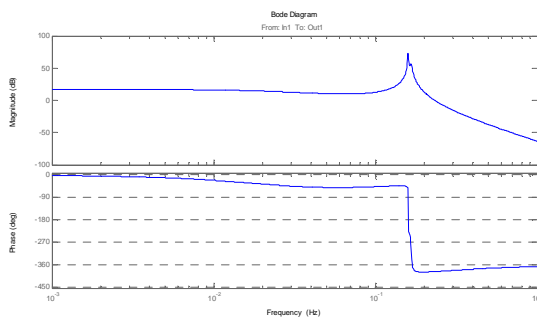


Figure 6-9 Bode Plot of Equation 6-3

From this analysis three things can be concluded about increasing the Mach number in the Steady Flow Model

1) Increasing Mach number has the same effect on the phase and amplitude as adding damping to the system.

2) For the forward traveling wave, to match the behavior, a second order system near the origin and a zero are required to match the shape of the amplitude and phase curves of the Steady Flow Model.

3) For the backward traveling wave, a damped second order system near the natural frequency, a zero and a pole are required to match the shape of the amplitude and phase curves of the Steady Flow Model

7 CONCLUSIONS AND RECOMMENDATIONS

Steady fluid motion has a three fold effect on wave propagation. First, the steady fluid motion, represented by Mach number, decreasing the natural frequency of the system. Second the fluid motion changes the phase behavior of the waves. For the Homogenous Wave Model the phase is -180 before the natural frequency and 0 after, with a 180 degree phase change at the natural frequency. For the Steady Flow model the forward and backward traveling waves exhibit variable phase through the entire range of frequencies. Third the amplitude of the backward wave is higher than that of the forward wave.

In three dimensional cylindrical combustors transverse waves will tend to spin in one direction instead of remaining steady. For cylindrical combustion systems with swirl, the different phase relationship of the forward and backward waves, as well as their differing amplitude may cause the waves to prefer to spin in one direction. According to the modeled data, this spinning behavior may even be true for low Mach numbers, ~0.1. The mode shapes in a two dimensional chamber with axial and transverse flow needs to be studied further to determine if this hypothesis is true. This phenomena should also be studied in the presence of loss mechanisms such as viscosity and damping added to the model.

A second peak appears when the boundary conditions are applied to the Steady Flow Model. To reproduce the forced response with transfer functions second order systems were required to

be added at the origin or near the natural frequency of the system. More study is required to determine if these second order systems are an artifact of the finite difference simplification, or if they are an artifact of the boundary conditions applied.

References

Dowling, A.P. and Stow, S.R., 2003, "Acoustic Analysis of Gas Turbine Combustors", *Journal of Propulsion and Power*, 19(5), 751-764.

Eversman, W., 1970, "The Effect of Mach Number on the Tuning of an Acoustic Lining in a Flow Duct Lining", *Journal of the Acoustic Society of America*, 48, 2, 425-428.

Eversman, W., 1971a, "The Effect of on the transmission and Attenuation of Sound in an Acoustically Treated Circular Duct", *Journal of the Acoustic Society of America*, 49, 5, 1372-1380.

Eversman, W., 1971b, "Signal Velocity in a Duct with Flow", *Journal of the Acoustic Society of America*, 50, 2, 421-425.

Gogate, G, and Munjal, M, 1992, "Analytical Solution of the Laminar Mean Flow Wave Equation in a Lined or Unlined Two-dimensional Rectangular Duct", *Journal of the Acoustical Society of America*, 92:5, 2915-2923.

Ingard, U., and Singhal, V., 1973, "Upstream and Downstream Sound Radiation into a Moving Flow", *Journal of the Acoustic Society of America*, 45, 4, 1343-1346.

Morse and Ingard, 1968, Theoretical Acoustics McGraw Hill, NY.

Ogata, K., 1970, *Modern Control Engineering*, Prentice-Hall.

Pota, H. R., and Kelkar, A. G., 2001, :Modeling and Control of Acoustic

Ducts", *Journal of Vibration and Sound*, 123, 2-11
Richardson, E. G., 1949, Sound, 2nd Edition, Edward Arnold and CO, London, p161-164.
Wood, A. B., 1957, A Textbook of Sound, 3rd Edition, Neill and Co. LTD, London, p179-182,

Appendix 1 Alternate Pressure Equation

Starting with the conservation form of the internal energy equation:

$$\frac{\partial(\rho e)}{\partial t} + \frac{\partial(\rho u e)}{\partial x} = -p \frac{\partial u}{\partial x} \quad (\text{A1-1})$$

For isentropic flow pressure, density and internal energy are related by:

$$\rho = \frac{p}{RT} = \frac{p}{e} \frac{1}{(\gamma-1)}; \quad \rho e = \frac{p}{\gamma-1}$$

Reducing equation A1-1 to:

$$\frac{\partial\left(\frac{p}{\gamma-1}\right)}{\partial t} + \frac{\partial\left(u \frac{p}{\gamma-1}\right)}{\partial x} = -p \frac{\partial u}{\partial x} \quad (\text{A1-2})$$

Assuming constant properties, equation A1-2 becomes:

$$\frac{1}{\gamma-1} \frac{\partial p}{\partial t} + \frac{1}{(\gamma-1)} \frac{\partial(up)}{\partial x} = -p \frac{\partial u}{\partial x}$$

Further manipulations:

$$\frac{\partial p}{\partial t} + \frac{\partial(up)}{\partial x} = (1-\gamma)p \frac{\partial u}{\partial x}$$

Applying the chain rule to the spatial derivative:

$$\frac{\partial p}{\partial t} + p \frac{\partial u}{\partial x} + u \frac{\partial p}{\partial x} = (1-\gamma)p \frac{\partial u}{\partial x}$$

$$\frac{\partial p}{\partial t} + u \frac{\partial p}{\partial x} = (1-\gamma-1)p \frac{\partial u}{\partial x}$$

The final pressure equation is:

$$\frac{\partial p}{\partial t} + u \frac{\partial p}{\partial x} = -\gamma p \frac{\partial u}{\partial x}$$

$$\frac{\partial p}{\partial t} + u \frac{\partial p}{\partial x} = -\rho a^2 \frac{\partial u}{\partial x} \quad (\text{A1-3})$$

Appendix 2 Alternate Momentum Equation

Starting with the momentum and continuity equations:

$$\frac{\partial \rho}{\partial t} = -\rho \frac{\partial u}{\partial x} - u \frac{\partial \rho}{\partial x} \quad (\text{2-1})$$

$$\rho \frac{\partial u}{\partial t} + \rho u \frac{\partial u}{\partial x} = -\frac{\partial p}{\partial x} \quad (\text{2-2})$$

Multiplying equation 2-1 by u and rearranging results in:

$$\rho u \frac{\partial u}{\partial x} = -u \frac{\partial \rho}{\partial t} - uu \frac{\partial \rho}{\partial x} \quad (\text{A2-1})$$

The derivatives of density are converted by the isentropic relationship for pressure and density:

$$\partial p = a^2 \partial \rho$$

Resulting in

$$\rho u \frac{\partial u}{\partial x} = -\frac{u}{a^2} \frac{\partial p}{\partial t} - \frac{uu}{a^2} \frac{\partial p}{\partial x} \quad (\text{A2-2})$$

The alternate momentum equation is obtained by substituting Equation A2-2 into Equation 2-2

$$\rho \frac{\partial u}{\partial t} = +\frac{u}{a^2} \frac{\partial p}{\partial t} + \frac{uu}{a^2} \frac{\partial p}{\partial x} - \frac{\partial p}{\partial x}$$

Grouping terms results in:

$$\rho \frac{\partial u}{\partial t} = \frac{u}{a^2} \frac{\partial p}{\partial t} + \left(\frac{uu}{a^2} - 1\right) \frac{\partial p}{\partial x} \quad (\text{A2-3})$$